Polarization-color mapping strategies: catching up with color theory

Andrew Kruse, Andrey Alenin, Israel Vaughn, J. Scott Tyo

Andrew W. Kruse, Andrey S. Alenin, Israel J. Vaughn, J. Scott Tyo, "Polarization-color mapping strategies: catching up with color theory," Proc. SPIE 10407, Polarization Science and Remote Sensing VIII, 104070G (25 September 2017); doi: 10.1117/12.2274254

SPIE.

Event: SPIE Optical Engineering + Applications, 2017, San Diego, California, United States

Polarization-color mapping strategies: catching up with color theory

Andrew W Kruse, Andrey S. Alenin, Israel J. Vaughn, and J. Scott Tyo*[a]
[a]University of New South Wales Canberra, Northcott Drive, Campbell ACT 2612, Australia;

ABSTRACT

Current visualization techniques for mapping polarization data to a color coordinates defined by the Hue, Saturation, Value (HSV) color representation are analyzed in the context of perceptual uniformity. Since HSV is not designed to be perceptually uniform, the extent of non-uniformity should be evaluated by using robust color difference formulae and by comparison to the state-of-the-art uniform color space CAM02-UCS. For mapping just angle of polarization with HSV hue, the results show clear non-uniformity and implications for how this can misrepresent the data. UCS can be used to create alternative mapping techniques that are perceptually uniform. Implementing variation in lightness may increase shape discrimination within the scene. Future work will be dedicated to measuring performance of both current and proposed methods using psychophysical analysis.

Keywords: Polarization, data visualization, color space, color map,

1. INTRODUCTION

When displaying polarization data, a common strategy is to map polarization parameters to color. The first contribution towards this strategy was a description of the similarities in polarization vision and color vision [1]. In Bernard and Wehner's work, , polarization parameters of angle (AoP) and degree (DoP) were shown to be analogous to the color parameters hue and saturation, respectively. In the same year, Walraven introduced polarization imaging as a widely applicable technique, also describing an analogy between polarization and color in a similar matter to Bernard and Wehner [2]. Shortly after this, more material foundational to the field of polarization imaging was contributed by Solomon that detailed the first specific methods for calculating color values that could represent the polarization parameters [3]. These methods were dependent on calculations using a color model developed by Faugeras [4]. The reasoning behind choosing this color model was that it was designed to be perceptually uniform, which means that the Euclidean distance between two colors in the 3D color space is meant to describe actual perceptual differences. Unfortunately for the widespread use of Solomon's mapping, Faugeras' color model was never widely accepted, perhaps because CIELAB, a functionally similar color model, was introduced by the International Commission on Illumination (CIE), the established authority on color modeling in the same year. Around the same time, the introduction of the Hue, Saturation, Value (HSV, also known as HSB with brightness instead of value) transformation of RGB triplets defined a convenient, computationally quick way to convert between cylindrical and Cartesian color coordinates, the latter of which is the default method of image color construction in monitors, computers, digital cameras, and the internet [5]. As such, it is not surprising that the first implementations of hue mapping for digital polarimetric images used the HSV transformations [6-8].

The wide usage of this method, along with the obscurity of Faugeras' color model, are likely reasons that Solomon's methods have evidently never been implemented.The potential benefits of perceptual uniformity of the mappings have not been revisited since Solomon's paper, even in the scarce literature that specifically discuss polarization display strategies [8-12]. The remainder of this paper is organized as follows. In section 2, a discussion on the non-uniformity and its potential effects on perception offers rationale for replacing HSV in favor of a uniform color model as the basis for polarization mapping. In section 3, the state-of-the-art uniform color space CAM02-UCS is used to implement a modern version of Solomon's mappings that is consistent with current color theory. While intuition would suggest that this new mapping strategy should perform better than the current HSV mappings using criteria derived from uniformity as well as other general visualization guidelines, section 4 will show the need for future work to determine validation from human perceptual testing.

Although much less common, implementations using Hue, Saturation, Lightness (HSL) [13] and purposefully discontinuous coloration [14-16] have been used throughout the literature. It is also noteworthy that colorful, non-periodic mappings included in software packages like MATLAB's "jet" are common for representing angle of polarization [17-

*a.kruse@student.adfa.edu.au;

Polarization Science and Remote Sensing VIII, edited by Joseph A. Shaw, Frans Snik,
Proc. of SPIE Vol. 10407, 104070G · © 2017 SPIE · CCC code: 0277-786X/17/$18
doi: 10.1117/12.2274254

19]. However, due to the discontinuity of the endpoints, these mappings are not functionally equivalent to periodic mappings. Thus, this paper will only be focusing on periodic mappings, and in particular, the HSV mapping.

2. NON-UNIFORMITY IN HSV

2.1 Perceptual changes with system rotations

Before discussing a practical measure of perceptual uniformity, it is advantageous to first start with a more intuitive and visual demonstration of how changes in the perception of polarimetric data can be caused by artifacts of non-uniformity. In this demonstration, one set of data is used to create two visualizations that are constructed from HSV mappings, where only the arbitrarychoice of the hue angle of zero differes. This rotation of hues would naturally come about from any of the following: a rotation of the polarimeter, a rotational movement of objects in the scene, or the arbitrary choice of system polarization coordinates. Furthermore, the angles of polarization will vary for a fixed camera-scene configuration as the illumination conditions vary.

In Figure 1, the two visualizations are contrasted side by side. Looking at the features indicated by the arrows, it is clear that the two visualizations are very much affected by the arbitrary rotation, with extreme differences in visibility of features, magnitudes of gradients, and the appearance of noise. Section 2.2provides a theoretical understanding for why the perceptual inconsistencies occur based on current color theory.

When perceptual inconsistencies are introduced into the mapping of data, there is an inherent risk in being presented with a false depiction of the information in the scene. There is no way to tell beforehand what parts of the scene are going to be exaggerated, what parts may be hidden, or what parts are displayed accurately. Clearly this is not ideal.

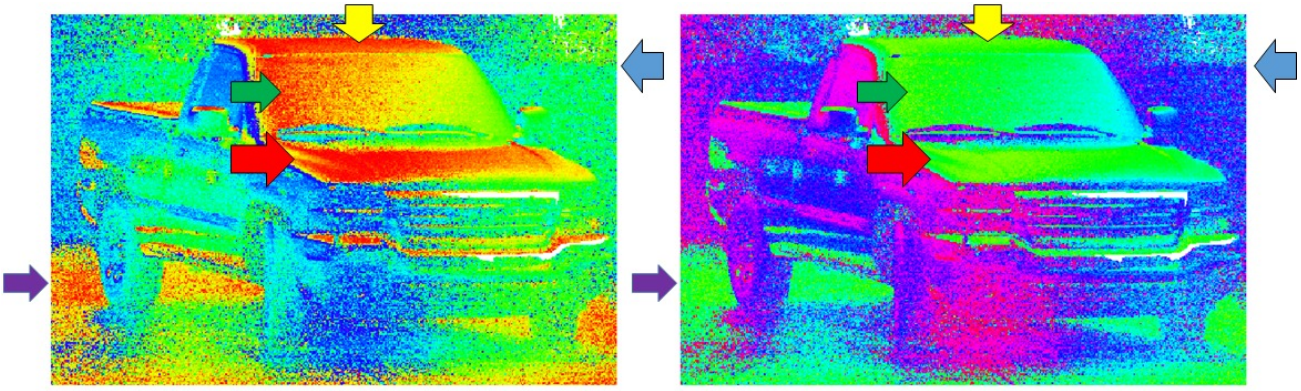

Figure 1. Comparison of different visualizations of the same AoP data using the HSV color model for hue. White indicates areas with no polarization data. The arrows indicate points of interest that are likely to be perceived differently. Each arrow is described in Table 1.

Arrow	Feature	Perceptual Difference
Yellow	Roof	Only visible in left image
Green	Windshield	Stronger gradient in left image
Red	Hood	Detail only visible in left image
Blue	Wall	Only visible in right image
Purple	Ground	More noisy in left image

Table 1. Perceptual differences between the left and right sides of Figure 1 for the features indicated by the colored arrows.

2.2 Measuring perceptual uniformity

In this section, the ability to analyze uniformity within a colormap is described using the metric ΔE_{UCS} of perceptual difference established by the CAM02-UCS (or simply UCS) color model [20]. The subscript UCS may not appear in the literature, but it is used here to differentiate between other measures of ΔE. Readers may be familiar with the ΔE concept

in describing perceptual or color difference, and in particular for CIELAB (ΔE^*_{ab}) or CIEDE2000 (ΔE_{00}). While these are all calculated differently, they all are used to describe the same concept in a similar way. In section 3.1, the merits of the UCS model will be discussed, which will give justification for its use in this section. In addition, the color calculations and plots will be using viscm: a 3rd party Python module developed to analyze and visualize mappings using color differences in UCS [21].

In Figure 2, the HSV colormap included in the matplotlib module is analyzed with the viscm tool. This tool calculates the perceptual variation between sequential colors within a given colormap. In this case, the x-axis is analogous to hue angle, divided into 256 steps. For each step, the UCS equivalent color of the sRGB triplet is calculated with

$$(J'_n, a'_n, b'_n) = sRGBtoUCS(R_n, G_n, B_n), \tag{1}$$

where *J', a', b'* are the UCS color coordinates, *R,G,B* are the sRGB values for red, green, and blue, and the subscript indicates the n^{th} step in the colormap. The function *sRGBtoUCS* represents the calling of a sRGB to UCS transformation function in the module colorspacious, which is a tool for converting between color spaces [22]. The y-axis is meant to represent a perceptual derivative, approximated by the normalized perceptual difference between sequential colors, given by

$$PD(n) = N \cdot \sqrt{(J'_n - J'_{n+1})^2 + (a'_n - a'_{n+1})^2 + (b'_n - b'_{n+1})^2} = N \cdot \Delta E_{UCS}(n, n+1), \tag{2}$$

where *PD* is the perceptual derivative as a function of the n^{th} step, and *N* is the number of steps in the colormap used to normalize the calculation for any arbitrary number of steps in the colormap. The actual values given by the perceptual derivative are only meant for relative comparison with other maps. Some other important metrics given are the sum of all non-normalized differences (Length), the standard deviation of the differences (RMS deviation), and the RMS deviation as a percentage of length. A uniform colormap, like the one described by Solomon, would have a constant perceptual derivative, while the derivative for a non-uniform map would be a function of hue angle. An effective strategy to creating a uniform map would therefore be to minimize the RMS deviation of the perceptual derivative.

2.3 Perceptual derivative of HSV mapping

Figure 2 shows an analysis of the uniformity of the HSV mapping using the method described in section 2.2The line traced by the perceptual derivative clearly does not follow a sensible path. The rate of change between steps is very small for the colors red, green, and blue, while it is much greater for yellow, cyan, and violet. It is therefore evident that the perceptual difference resulting from an angular difference in hue is dependent on the hue angle. Referring again to Figure 1, the inconsistencies between the images matches what would be predicted by examining Figure 2. Features defined by small differences in polarization angle have degraded visibility when they fall within the green range. This would be predicted by the wide region of lower rate of perceptual change associated with the green range. Similarly, features that contain yellow, cyan, and purple can have heightened visibility, which would be predicted by the high rates of change for those colors.

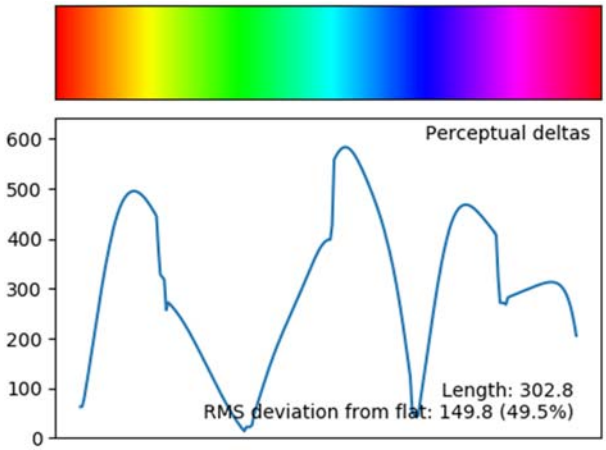

Figure 2. Visualization of perceptual non-uniformity using viscm Python module. The y-axis indicates perceptual derivative given by Equation 2 . The x-axis is just the sequence of colors and therefore not labeled with values. Rather, the colormap above the plot roughly shows the corresponding colors.

2.4 Other non-uniformities in HSV

In this section, the UCS definitions of hue angles, colorfulness, and lightness that are discussed can be found in more detail in section 3.1, but for the purposes of this section may be thought of as perceptually uniform versions of hue, saturation, and value from HSV. Figure *3* shows how these variables change non-uniformly for the HSV mapping. In the polar plot, it can be seen that each dot representing a uniform change in HSV hue angle is not uniformly spaced in UCS hue angle. In particular, the separations in hue become very small for regions around red, green, and blue, which agrees with the plot of Figure 2. The large markers indicate the 6 main colors of HSV: red, yellow, green, cyan, blue, and magenta. If the hues were to be perceptually uniform, these markers would line up equally spaced at 60° apart in UCS, but they are not. In terms of finite steps within the colormap, there are just as many steps between the red and yellow markers as there are between the yellow and green. The perceptual hue difference is 2.4 times greater for red to yellow than yellow to green, yet are mapped with the same amount of steps. Also included in this plot is a histogram of steps in each 30° bin out of a total of 256 steps. This is analogous to the probability distribution for each hue range. In polarization terms, for a random polarization angle, the hue it would be mapped to is much more likely to be green (UCS hue 120°-150°) or blue (UCS hue 240°-270°) than any other hue. For an ideal colormap, the probability of any hue should be uniform. This non-uniformity indicates that the perception of hues do not accurately represent the actual values in the data.

For the lightness plot, the non-uniformity is clear. For some hues, the lightness changes rapidly, while for others it does not change much at all. In section 3.3, the importance of lightness variation on shape discrimination is discussed. For this HSV mapping, this could mean that shape discrimination is much easier for particular color combinations. For example, since the lightness of blue (HSV hue 240°) is much lower than its surrounding colors, areas with a polarization angle that gets mapped to blue would likely be the easiest to discriminate from the background. Figure 1 and Figure 8 are good examples of how well blue defines shapes in HSV mappings. In contrast, areas with a polarization angle that gets mapped to an area of similar lightness to the background may not be easily distinguished. For example, combination of green/cyan as well as magenta/red do not appear to define shapes well in Figure 8

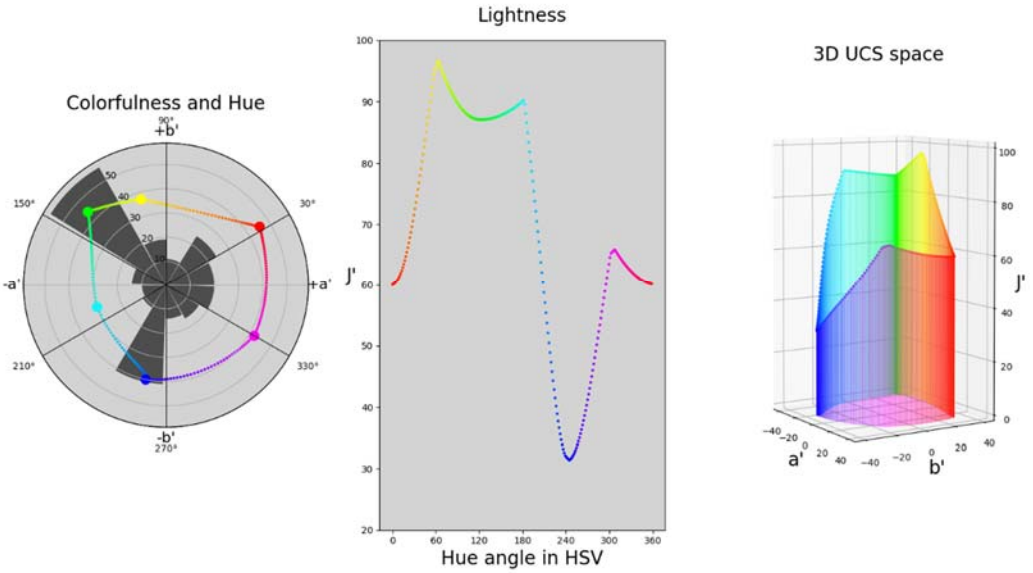

Figure 3. Color properties of the HSV mapping of size 256 steps are plotted. Each step is plotted as a single point with its corresponding color. Left: polar plot of colorfulness and hue, with large markers indicating the primary and secondary colors red, yellow, green, cyan, blue, and magenta. These 6 colors are equally spaced in hue angle in HSV, but not in UCS. Black lines indicate where markers should roughly be if spaced uniformly. Dark gray bars indicate number of discrete steps that fall within that perceptual hue range. Radius ticks correspond to both colorfulness for the dots and the histogram count for the bars. Center: plot of lightness. Right: 3D representation of the perceptual curve with projection to $J' = 0$ plane.

2.5 Variation in perceptual difference

In addition to the UCS distance metric, color differences can be measured by a metric called ΔE. The current standard for calculating ΔE is given by the CIEDE2000 formula, and distinguished from other definitions by labeling it ΔE_{00} [23]. This standard is built on the CIELAB model instead of CIECAM02, and thus will provide a slightly different value than the UCS distance. More information on the difference in the two different color difference metrics is provided in section 3.1; however, in this section, the HSV colormap will be analyzed using both metrics.

The range of perceptual differences between all possible two color combinations that represent a set angular difference can be determined. With a non-uniform mapping, it would be expected that for a given angular difference, there would be variation in the perceptual differences that depended on the color combination. In addition, the variation may behave nonlinearly with respect to angular difference. In contrast, a perfectly uniform mapping would show no variation in perceptual differences and would have a perfectly linear relationship between angular and perceptual difference. However, due to the periodic necessity of this mapping, it is not possible to create this linear relationship.

In Figure 4, this range of perceptual differences is plotted for the full domain of polarimetric angular differences, from parallel to perpendicular, using both color difference metrics. For each polarimetric angular difference, the color combinations yielding the greatest and least perceptual differences are plotted, with one color as the background and one as the edge and texture for visual reference. As expected, the relationship between polarimetric angular and perceptual difference is both nonlinear and highly varying. Following the curve of the greatest difference using either metric, it immediately diverges from the curves of the mean and the least difference. In contrast, the curve of the least difference takes much longer to increase. One way to identify perceptual non-uniformity is to compare the values of the curves at a given polarimetric angular difference. The range between the greatest and least curves describes how differently that angular difference could be perceived, depending on the color combination. For example, at a 20°difference, the greatest perceptual difference is about twice as large as the mean for both metrics, and either 8 times the least for the ΔE_{UCS} or 11 times for ΔE_{00}. Even considering only the range of 1 standard deviation from the mean at 20° difference, the upper bound has a perceptual difference of more twice the lower bound for ΔE_{UCS} and 3 times for ΔE_{00}.

Another way to look at this plot is to compare the range of angular differences at a set perceptual difference. For example, a ΔE_{UCS} of 70 can result from anything between a 30° or a 90° angular difference. In addition, any angular difference greater than 30 degrees has the potential to have a higher perceptual difference than a 90° difference. Using ΔE_{00}, a similar result can be seen, and the range is even more dramatic. The ΔE_{00} value for a 90° difference could also result from a 20° difference. Any angular difference greater than 20° can similarly result in a greater ΔE_{00} color difference than a 90° difference.

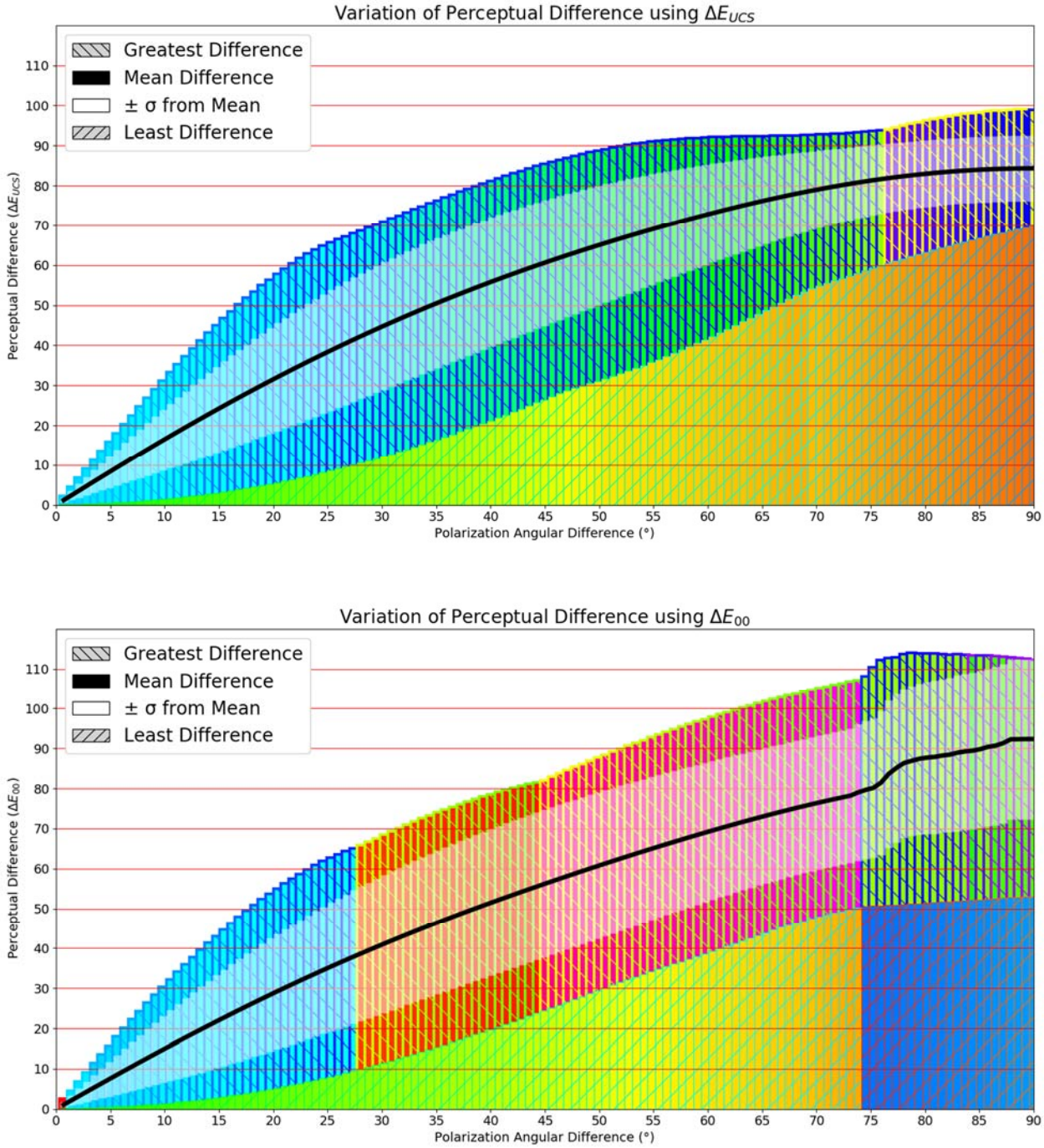

Figure 4. Plot of the range of perceptual difference for a given polarization angle difference. For each polarization angle difference, the perceptual difference of each possible color combination is calculated using a color difference formula. Top: the perceptual difference is ΔE_{UCS}. Bottom: perceptual difference is ΔE_{00}. The perceptual differences for the combinations that measure the greatest, the least, and the mean (with ± 1 st dev) difference are plotted. For the greatest and the least series, the color combinations are displayed with one color as the bar background color, and the other as the edge and texture color.

2.6 The problem with green

In Figure 4both metrics show the curve of least difference increasing at a very slow rate at small angular differences, and that this is associated with the color green. In addition, the curve for the greatest difference levels off in larger angular differences where green is one of the two colors in the color combination. For the ΔE_{UCS} metric, this occurs in the range of approximately 50° to 75° difference, and in the ΔE_{00} metric from a 75° to 90° difference. This could be predicted from the low value for the perceptual derivative in the green range according to Figure 2. In addition, the small variations that become virtually indistinguishable in Figure 1 are often due to this issue with the color green.

In order to understand just how small the perceptual difference in the least difference curve is for small angular differences(referred to here as the "green zone") it is useful to use the concept of a "just noticeable difference" (JND). The JND threshold is the amount of color difference necessary for a normal observer to perceive a difference between two colors. A color difference of 1, when calculated using formulas used in this paper (ΔE_{UCS}, ΔE_{00}), is often used as a rough estimate of the JND threshold. However, getting an empirical, definitive relation of the perceptual difference units to JND is so difficult that it is not even attempted [24]. For CIELAB color space, a value of 2.3 ΔE^*_{ab} has been discussed [25]. However, the source for this value had an uncertainty of 1.3 ΔE^*_{ab}, and did not even mention the value in relation to JND but instead as a way to relate base units of various color spaces [26]. Similar studies have not been done on CIEDE2000 or CAM02-UCS. Therefore use of the base unit of color difference as JND in this paper is admittedly a very simplified approximation.

In Figure 5, the perceptual difference in the green zone only reaches the JND threshold at an angular difference of around 8.0° for ΔE_{UCS} and 8.4° for ΔE_{00}. Angular differences less than this may be impossible to be detected by a human observer when mapped in the green zone. Even at a 14.0° difference, the two colors in the green zone are still too difficult to distinguish without close examination. In contrast, the mean perceptual difference is already above the JND threshold at a 0.7° difference, which is the smallest angular difference possible in a map of 256 colors.

3. DEFINING A PERCEPTUALLY UNIFORM COLOR MAPPING

3.1 CAM02-UCS

In this section, the uniform color space based on the color appearance model CIECAM02 (CAM02-UCS or just UCS) will be discussed. In 2006, three uniform color spaces were introduced based on the data set they were meant to fit: data comprised of large color differences (LCD), small color differences (SCD), and the combined data (UCS) [20]. Further analysis of these color spaces has shown robustness of the UCS model for performance of predicting both large and small color differences [27]. In addition, that study also suggested the use of CIEDE2000, with units $\Delta E_{00,}$ as an alternative method of predicting color difference for colors of various magnitudes. However, CIEDE2000 is not a color space, but rather a metric of color difference. In contrast, UCS is both a color space and a metric for color difference (ΔE_{UCS}).

Like CIELAB, UCS has three Cartesian axes, with one for lightness, and two for color. *J'* is the uniform fitting of *J*, the lightness value in CIECAM02. The color axes *a'* and *b'* are derived from the CIECAM02 cylindrical values of colorfulness *M* and hue *h*. The axes of *a'* can generally be thought of as the scale of redness to greenness, with positive values being redder and negative being greener. Similarly, *b'* would be the scale of yellowness to blueness, with positive values being yellower and negative being bluer. In cylindrical coordinates, UCS coordinates of radius and angle can also be defined by colorfulness *M'* and hue *h*, respectively. Note that hue is the same for both CIECAM02 and UCS, whereas colorfulness is weighted to be uniform in UCS. In addition, it is important to understand the difference between colorfulness and saturation. According to the International Lighting Vocabulary standard published by CIE, colorfulness is the "attribute of a visual perception according to which the perceived color of an area appears to be more or less chromatic" [28]. Saturation is the "colorfulness of an area judged in proportion to its brightness" [29]. Two colors with different levels of brightness could have the same amount of saturation but a different amount of colorfulness. Since UCS uses *lightness* instead of *brightness*, saturation does not easily come out from the coordinates, and it is thus much simpler to discuss colorfulness instead.

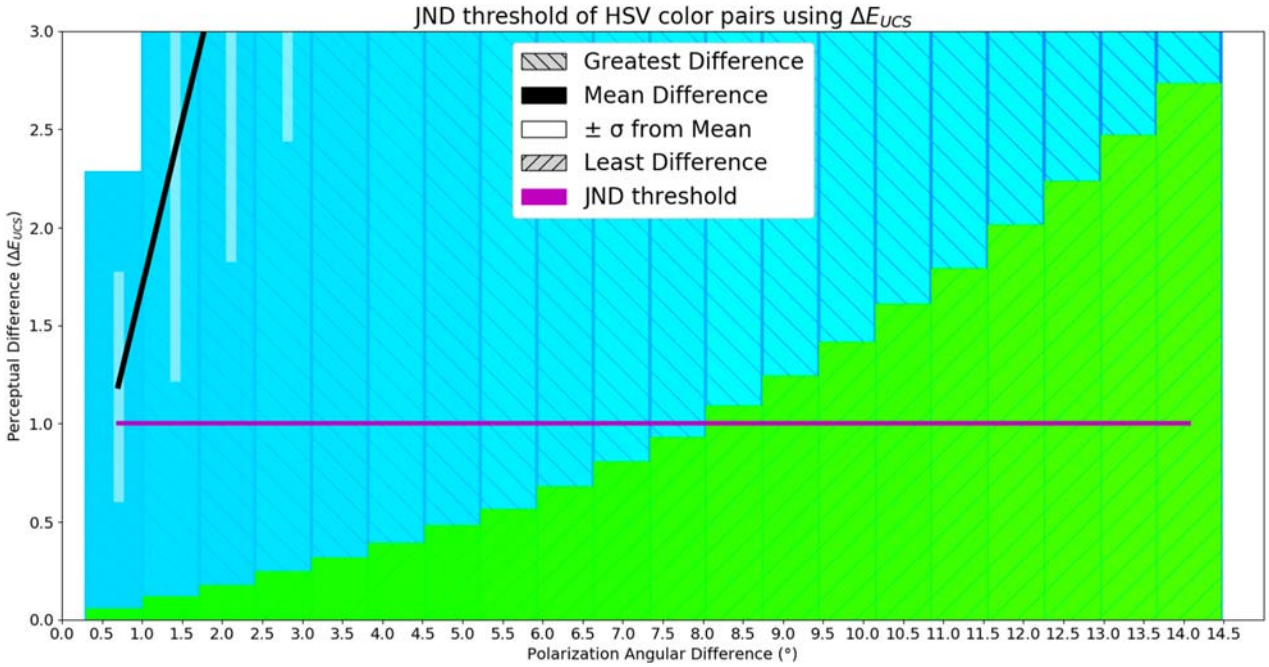

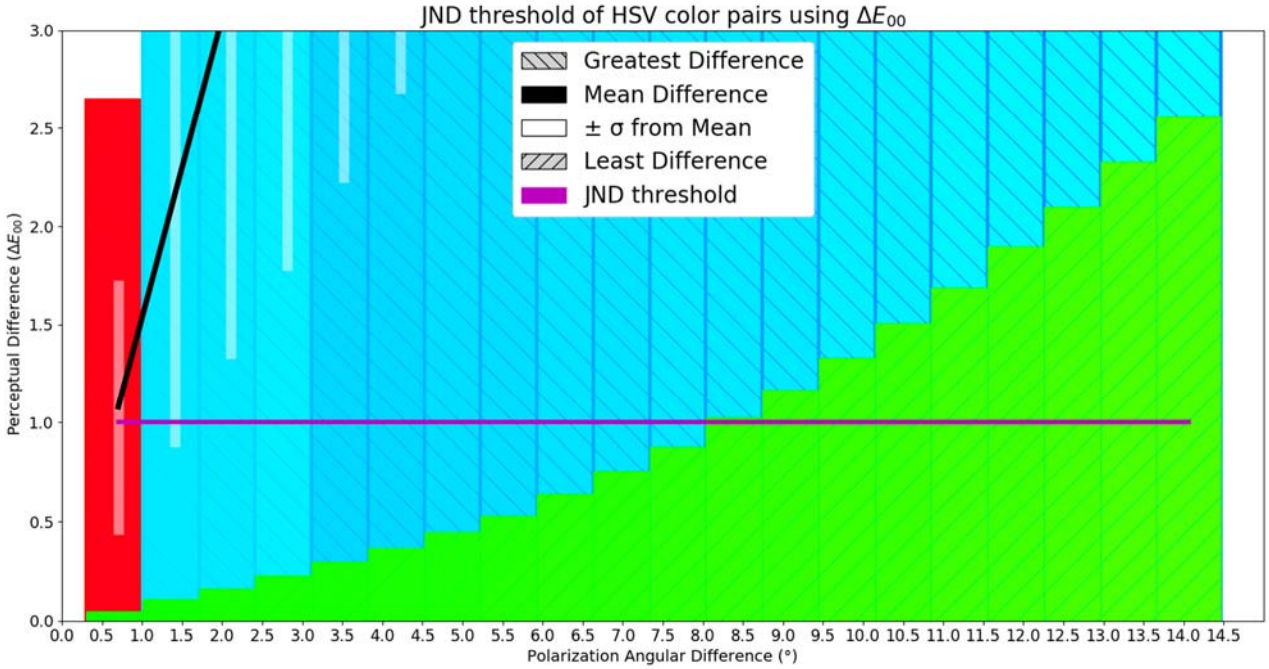

Figure 5. Same as Figure 4, but zoomed in to display the JND threshold. Note: both greatest difference and mean series extend further than the y-axis limit.

3.2 Mapping polarization into UCS

With these coordinates, it may seem straightforward to redefine the methods discussed in section 1 where the polarization parameters of normalized intensity, degree, and angle (*I, P, A*) to the UCS cylindrical coordinates of lightness, colorfulness, and hue (*J'*, *M'*, *h*).

$$I \rightarrow J', \quad P \rightarrow M', \quad 2 \cdot A \rightarrow h. \tag{3}$$

However, since the range of colorfulness is dependent on the lightness and hue,the mapping of *P* to *M'* is not so straightforward. The shape of the volume of total colors is not a cylinder like for HSV. For all lightness levels, there is always a gray color that exists where *M' = 0* so that a *P* value of 0 can be represented. In order for *P* values greater than 0 to uniformly correspond to an *M'* value, there needs to be a value of *M'* that corresponds to *P*=1. Simply taking the maximum *M'* value that exists within the volume at a given hue and lightness could give the scaling factor *k* such that

$$k_{J',h} P \rightarrow M', \qquad k_{J',h} = M'_{max}(J', h). \tag{4}$$

This method would utilize the entire volume of UCS, but would suffer from *P* values being mapped non-uniformly to *M'*, which would introduce many of the same issues addressed in section 2. Another mapping could be obtained by defining a subset of UCS by cutting out a cylinder with radius *k* and height J'_{max}, the lightness limit, with center *M' = 0*, and then implementing Equation 3. A major issue with this approach is that the radius would be incredibly small due to the shape of the UCS volume, where the range of *M'* approaches 0 as *J'* approaches both fully dark and fully light. This can be overcome by setting upper and lower bounds of *J'*, where the lightness levels allow for a wider range of colorfulness. However the drawback to this is losing the full range of lightness.

The solution to mapping the three polarization parameters into a uniform color space is not as simple a task as suggested by Solomon. In the future, we hope to define a mapping method that optimizes over the following criteria: uniformity, range of lightness, and range of colors (or colorfulness). In addition, there may be a benefit to including the polarization angle variability metric Δ, which was designed for increasing visibility of regions of low irradiance and high polarization, in the mapping method [30]. It is also important to recognize that the gamut of colors able to be displayed in monitors or print is only a subset of the full UCS volume. Since sRGB is the standard for display technology, it is of practical importance that the mappings are limited to the sRGB gamut, which is itself only a discrete set of colors (2^{24} for 24-bit true color. The subset of UCS defined by the sRGB gamut will be denoted UCS_{sRGB}. There is not much use for developing a mapping strategy in which the colors are not able to be adequately displayed as designed.

3.3 Polarization angle to hue for single variable mapping

In section 3.2, all 3 standard polarimetric parameters are discussed for mapping into UCS, however the focus will be shifted to the simpler problem of displaying polarization angle with hue for single variable mapping. In effect, any implementation is nearly identical to mapping angle to a 360° color wheel, with the exception that $2 \cdot A \rightarrow h$. In HSV, this wheel is created by setting value and saturation to full, and then using the full range of hue angles. In UCS, there is not a direct analogy between HSV variables value and saturation to UCS variables lightness and colorfulness. A color wheel of constant lightness and colorfulness can instead be constructed by first choosing a lightness value and then parametrizing a circle of constant colorfulness centered at *M'=0*. Choosing a lightness value gives a cross section where the range of colorfulness varies by hue. Thus there will be some limiting hue where the colorfulness range becomes the edge that circumscribes the circle. This maximizes the colorfulness of the wheel without having any color outside of the chosen gamut. The lightness value should be chosen so that the radius of the circle is large enough to include a wide range of colors.

A similar method has been briefly mentioned in recent developments in data visualization that utilize the uniformity of UCS color space for the development of new colormaps [31]. However, this implementation chose an arbitrary radius, which would indicate that the colorfulness was not necessarily maximized. In addition, this circular map was not included with the changes to the default colormaps in matplotlib v 2.0. The colormap library cmocean, which has been released on many platforms, also utilizes UCS and includes a periodic map called “phase” [32]. This map differs from the previously discussed in that the colorfulness is not a constant value, but approximately follows a smooth path closer to the edge of the lightness cross section. This means that some hues appear more colorful, which may inadvertently highlight angles and areas that are not especially significant. Future work outlined in section 4.2 will be aimed at measuring performance of this map and ones designed for this paper.

This technique was used to construct several color wheels from J'=50 to J'=70. The lightness level J'=70 allowed for the maximum radius at M'=25.8. In Figure 6, this color wheel is displayed in both the standard 360° "full circle" and in the 180° rotationally symmetric for polarimetric applications. Looking at the color wheels, two criteria for a good colormap are immediately evident: they are uniformly varying as well as colorful. In Figure 8 B/E, this map was applied to the same data as in Figure 1. It can be seen in this image that this mapping unfortunately does not seem to provide a high level of visual shape discrimination. While large color differences allow for easily distinguishable features (front window compared to side window), the subtler details are quite difficult to see (side of the truck).

This may be explained by the poorer performance for chromatic contrast than achromatic in shape discrimination tasks [33, 34]. By constraining the variation of the colormap in only hue, the benefits of achromatic contrast for shape discrimination are not available. Since variation in lightness occurs in virtually all natural scenes, allowing for achromatic contrast may allow the pseudocolor image to appear more like a natural scene. In polarimetric imaging, shape discrimination is an important feature that allows different polarimetric aspects (angle, degree, intensity) to be compared locally. When split into single variable maps, often by intensity, degree, and angle, it is essential for the shape discrimination to be maintained in order to compare features side by side. The difficulty in shape discrimination in current mapping strategies has been discussed in recent literature [12]. In the case of the cmocean "phase" map, the type of data it is meant to represent is slow variations such as wind or ocean currents, where shape discrimination is not an essential feature.

3.4 Implementation of lightness variation

It is with the intention of increasing shape discrimination that the constraint on constant lightness can be removed. Using parametrization of a circle tilted into the lightness axis, different colormaps can be created with varying lightness while retaining uniformity. The orientation of the circle can be defined by the tilt (zenith angle $\varphi \in [0, \pi]$) and the hue direction of the tilt (azimuth angle $\theta \in [-\pi, \pi]$). The hue direction can also be thought of as the hue corresponding to the peak lightness. Parametrization of the circle in 3D Cartesian coordinates using those spherical orientation angles is given by

$$P(\alpha) = R\cos(\alpha)\,\vec{u} + R\sin(\alpha)\,\vec{n}\times\vec{u} + C \tag{5}$$

$$\vec{n} = \begin{pmatrix}\cos\theta\sin\varphi\\ \sin\theta\sin\varphi\\ \cos\varphi\end{pmatrix},\quad \vec{u} = \begin{pmatrix}-\sin\theta\\ \cos\theta\\ 0\end{pmatrix},\quad \vec{n}\times\vec{u} = \begin{pmatrix}\cos\theta\cos\varphi\\ \sin\theta\cos\varphi\\ -\sin\varphi\end{pmatrix},\quad C = \begin{pmatrix}J'_C\\ 0\\ 0\end{pmatrix} \tag{6}$$

where P is a point on the circle, α is the parameter, R is the radius of the circle, $\vec{n}$ is the vector normal to the plane of the circle, $\vec{u}$ is the unit vector orthogonal to $\vec{n}$ in the a'-b' plane in the direction of θ, and C is the center of the circle, which is a gray point with lightness J'_C. The radius is maximized to fit within the sRGB gamut of the UCS space and will depend on the orientation and center of the circle. The parametrization thus has 3 degrees of freedom: J'_C, θ, φ. The shape of the UCS_{sRGB} volume offers an intuitive sense of the set of values that would yield a wide range of colors. For example, the space where the colorful blues resides is low in lightness (sRGB = [0,0,255] corresponds to $J' \approx 30$). On the other side, the colorful yellows and greens are in the upper range for lightness (sRGB = [0,255,0] and [255,255,0] correspond to $J' \approx 87$ and 97 respectively). Thus, in order to get those colors, J'_C, θ, and φ can be chosen to be oriented towards those points. Similarly, choosing the opposite θ so that the circle is tilted towards the light blue would likely result in a smaller range of values.

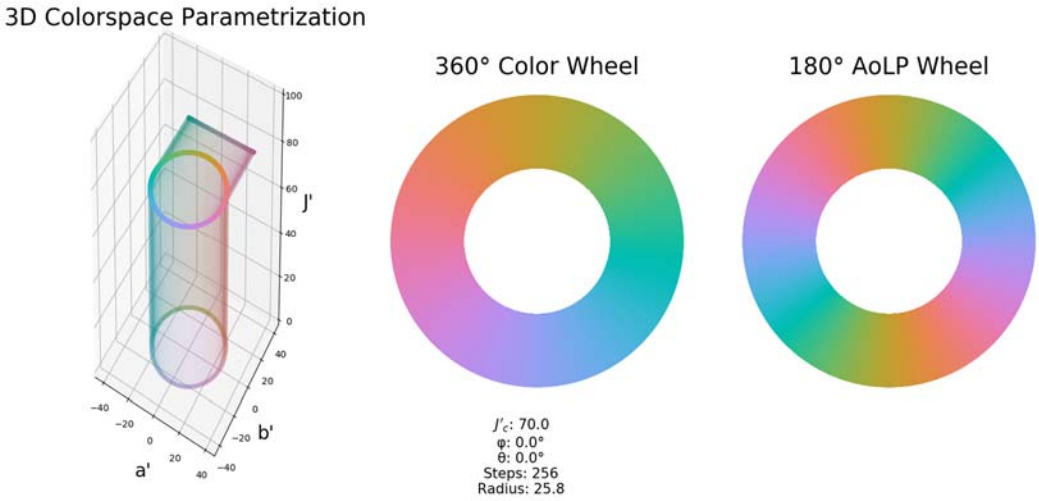

Figure 6. Colormap made from constant lightness and colorfulness in UCS. Left: 3D plot of parametrized circle with projections onto $J' = 0$ and $b' = 45$ planes. Center: standard 360° color wheel. Right: Polarization angle color wheel with 180° rotational symmetry.

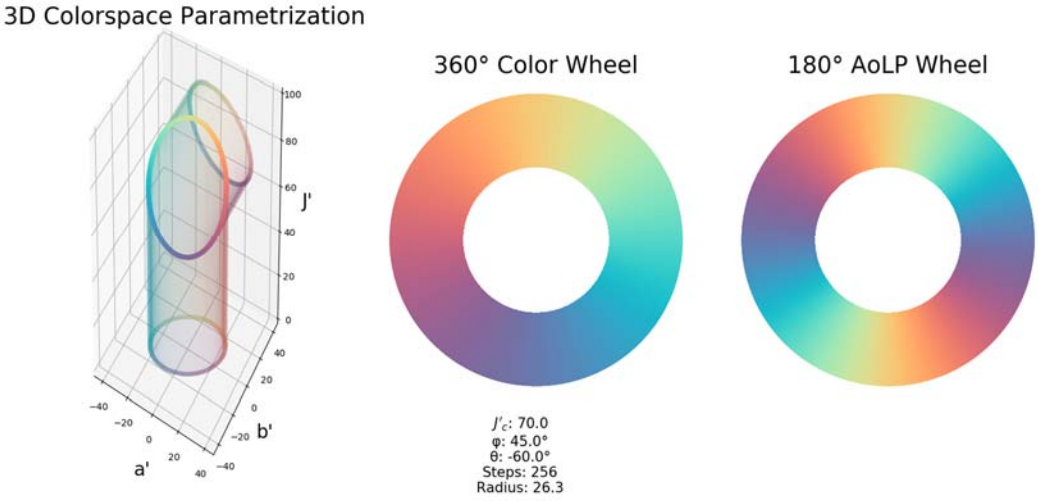

Figure 7. Colormap made from varying lightness and colorfulness in UCS. Left: 3D plot of parametrized circle with projections onto $J' = 0$ and $b' = 45$ planes. Center: standard 360° color wheel. Right: Polarization angle color wheel with 180° rotational symmetry.

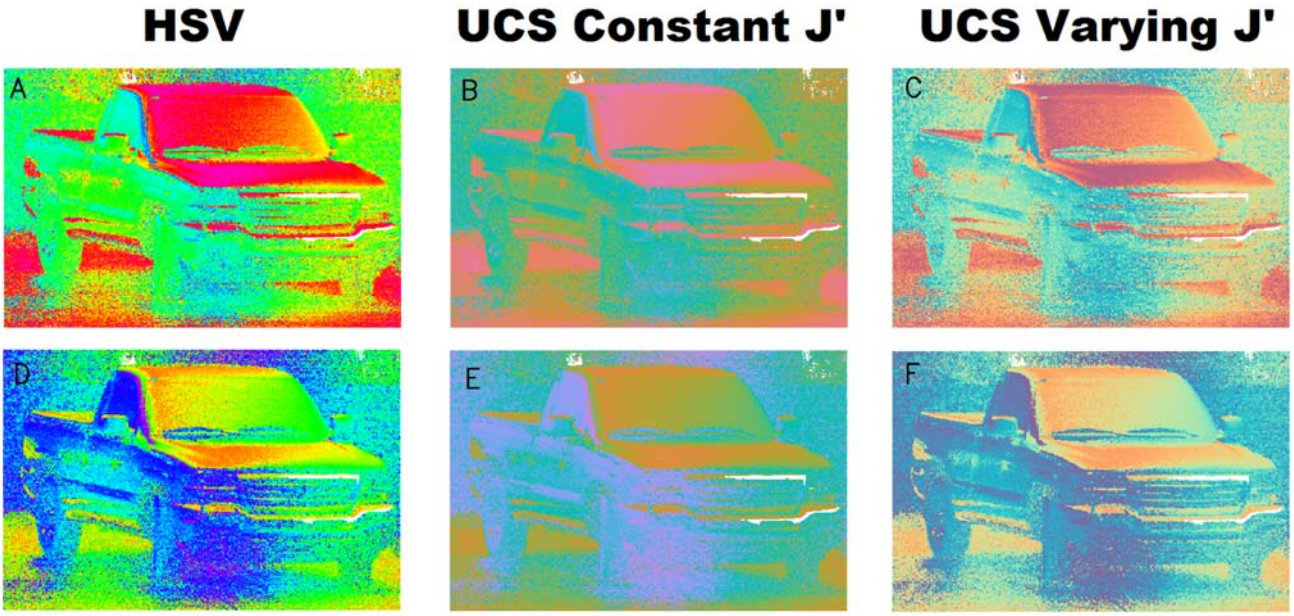

Figure 8. Polarization angle image constructed using different colormaps. White indicates areas with no polarization data. A/D: HSV with full saturation and value, B/E: Constant lightness and constant colorfulness in UCS, C/F: Added variation in lightness in UCS. Each row is at corresponds to a hue rotation so that the hues match for each method. Data collected using the IHIP polarimeter by J. M. Craven [35].

Using different combinations of the variables, dozens of new colormaps were created. Generally, the maps we preferred went along with our intuition for orienting upwards toward yellow-green. In Figure 7, a colormap made with the same center lightness as the one in Figure 6 is displayed. This map was chosen because of its similar radius to the flat lightness map so that the difference in shape discrimination can be attributed to the lightness variation. In Figure 8, side by side comparison of the other maps demonstrates the increase in shape discrimination performance.

In earlier work [30], we introduced a colorimetric mapping for use with both visible and infrared data that uses the local spatial statistics of polarization angle as a metric of confidence. In regions where the variance of the angle of polarization is high, we assumed that the polarization data were unreliable. In regions of low angular variance, we assumed that we had good confidence, even if DoLP was low. In these regions, we were able to apply strong amplification to the data to highlight regions of robust polarization and reveal areas that were otherwise hidden. Figure 9 shows a comparison of this mapping strategy using the original HSV mapping and the CAM02-UCS mapping proposed here.

4. FUTURE WORK: PERCEPTUAL TESTING

4.1 Optimization of lightness variation

In section 3.4, the method for allowing lightness variation discussed the three degrees of freedom for orienting a color wheel within UCS_{sRGB}. Although some choices of variables may intuitively seem much more likely to produce an effective mapping strategy, the optimization of the three variables is still undetermined. The most appropriate method for determining the optimum set of values would be to perform psychophysical experiments. The performance metrics of these tests would quantitatively describe the attributes of the given colormap such as uniformity and shape discrimination. The experiments should assess how each variable affects performance in given tasks for a wide variety of scenarios. Possible tasks include assessing the perceived difference corresponding to angular differences, identifying angular values corresponding to colors when given a color wheel, or comparing change of appearance of objects in a scene when hues are rotated (e.g. comparing objects in the left and right sides of Figure 1).

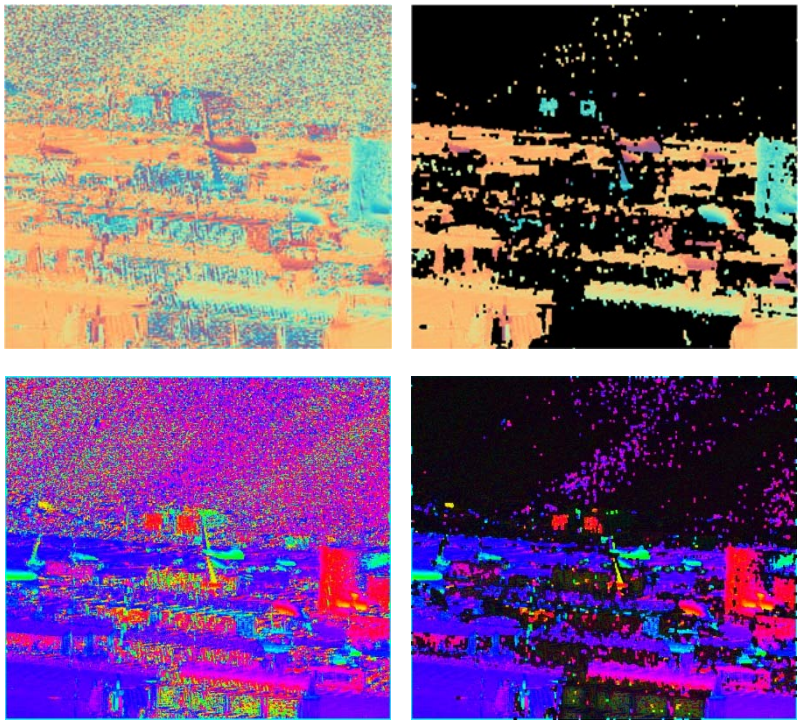

Figure 9. Implementation of the color mapping of Tyo, *et al*, [30] where regions of low confidence have been suppressed.

Another interesting option could be to remove the constraint of perfect uniformity in favor of increased performance for shape discrimination. Since the visual system has an inherent bias towards achromatic contrast for shape discrimination compared to chromatic, it may be advantageous to allow for some ellipticity in the parametrization, with the major axis in the plane of constant lightness. This would introduce some non-uniformity as a tradeoff for higher shape discrimination. Verification of this could be achieved through the psychophysical experiments.

4.2 Comparison to other methods

While the shortcomings of the current methods and potential remedies of the proposed methods are evident, it is important to remain cautious with proceeding with any attempts to change the default method. The effort required to change practices has to be matched by a quantitative performance increase for the sake of practicality. While we have little doubt that the proposed methods would perform better than the current methods, the extent of the performance increase is uncertain before any psychophysical experimentation. Currently, both HSV and cmocean's "phase" maps are available across many platforms, so there would need to be evidence of significant performance difference to justify forgoing the usage of tools already available.

5. CONCLUSION

While mapping polarization parameters to color has been a very interesting and useful tool, it is important to make sure the specific technique accurately represents the information in the scene. Even at the early stages of this technique, perceptual uniformity of the color space was described by Solomon an essential feature for achieving this [3]. However, due to possible factors such as limited computational power, prevalence of HSV, and obscurity in the Faugeras color space, Solomon's method never reached popularity within the polarization community. Although HSV is a convenient color space to use for mapping polarization, its inherent non-uniformity may have adverse effects leading to misrepresentation of data. For hue, non-uniformity means perceived differences in hue do not reflect the same difference in polarization angle. Particularly for green hues, an angular difference in polarization can appear much smaller or even

nonexistent. For lightness, non-uniformity means unintentional variation in shape discrimination with high dependence on the specific polarization angles. In addition, the amount of perceived difference in any two HSV hues that represent a polarization angular difference is so inconsistent that perceived difference cannot accurately describe polarization angular difference.

The uniform color space UCS offers the ability to create alternatives to the mapping techniques so that polarization visualization is consistent with current color appearance models. A parametrized circle in 3D UCS space forms a color wheel that maps angles to hue uniformly as an alternative to the HSV definition of hue. Initially, this was done at a set lightness, however this did not produce an image with good shape discrimination. Since lightness variation is an important cue for shape discrimination, the constant lightness constraint was removed. The circle can be parametrized so that it is tilted in lightness, creating variation, without losing uniformity. Optimization of the parametrization parameters has yet to be determined, however the benefits of shape discrimination are apparent from an intuitive choice of parameters. Future work will be aimed at implementation of psychophysical tests for both optimization of parameters and measurement of the actual difference in performance of current and proposed methods. A demonstration of the extent of performance differences would be necessary to justify advocating alternatives to the current methods.

REFERENCES

[1] G. D. Bernard, and R. Wehner, “Functional similarities between polarization vision and color vision,” Vision Research, 17(9), 1019-1028 (1977).

[2] R. Walraven, "Polarization imagery." *Proceedings of SPIE, vol. 112, Optical Polarimetry: Instrumentation and Applications*, pp 164 - 167,(1977)

[3] J. E. Solomon, “Polarization imaging,” Applied Optics, 20(9), 1537-1544 (1981).

[4] O. D. Faugeras, [DIGITAL COLOR IMAGE PROCESSING AND PSYCHOPHYSICS WITHIN THE FRAMEWORK OF A HUMAN VISUAL MODEL] The University of Utah, Ann Arbor(1976).

[5] A. R. Smith, “Color gamut transform pairs,” SIGGRAPH Comput. Graph., 12(3), 12-19 (1978).

[6] L. B. Wolff, and T. A. Mancini, "Liquid crystal polarization camera." *Proceedings of the IEEE conference on computer vision and pattern recognition*,"Liquid crystal polarization camera." pp. 120-127 (1992).

[7] L. B. Wolff, “Polarization camera for computer vision with a beam splitter,” Journal of the Optical Society of America A, 11(11), 2935-2945 (1994).

[8] J. Tyo, E. Pugh, and N. Engheta, “Colorimetric representations for use with polarization-difference imaging of objects in scattering media,” JOSA A, 15(2), 367-374 (1998).

[9] K. M. Yemelyanov, S.-S. Lin, W. Q. Luis *et al.*, "Bio-inspired display of polarization information using selected visual cues." *Proc. SPIE vol. 5158: Polarization Science and Remote Sensing*, pp. 71-84 (2003).

[10] F. Snik, J. Craven-Jones, M. Escuti *et al.*, "An overview of polarimetric sensing techniques and technology with applications to different research fields." *Proc. SPIE vol 9099*: *Polarization Measurement, Analysis, and Remote Sensing XI* , pp. 90990B-90990B-20 (2014).

[11] D. A. Lavigne, M. Breton, G. Fournier *et al.*, "Target discrimination of man-made objects using passive polarimetric signatures acquired in the visible and infrared spectral bands." *Proc. SPIE vol. 8160:Polarization Science and Remote Sensing V* , pp. 816007-816007-9 (2011).

[12] Y. L. Gagnon, and N. J. Marshall, “Intuitive representation of photopolarimetric data using the polarization ellipse,” Journal of Experimental Biology, 219(16), 2430-2434 (2016).

[13] S. b. Breugnot, and P. Cle´menceau, “Modeling and performances of a polarization active imager at λ=806 nm,” Optical Engineering, 39(10), 2681-2688 (2000).

[14] G. Horváth, J. Gál, I. Pomozi *et al.*, “Polarization Portrait of the Arago Point: Video-polarimetric Imaging of the Neutral Points of Skylight Polarization,” Naturwissenschaften, 85(7), 333-339 (1998).

[15] R. Hegedüs, S. Åkesson, R. Wehner *et al.*, "Could Vikings have navigated under foggy and cloudy conditions by skylight polarization? On the atmospheric optical prerequisites of polarimetric Viking navigation under foggy and cloudy skies." *Proc. Royal Society A* vol. 463, pp. 1081-1095 (2007)

[16] A. Barta, A. Farkas, D. Száz *et al.*, “Polarization transition between sunlit and moonlit skies with possible implications for animal orientation and Viking navigation: anomalous celestial twilight polarization at partial moon,” Applied Optics, 53(23), 5193-5204 (2014).

[17] L. Patrick, M. Graham, and P. Stanley, “Lens array Stokes imaging polarimeter,” Measurement Science and Technology, 22(6), 065901 (2011).
[18] E. Vexberg, and M. A. Golub, "Optical imaging system which is sensitive to a degree of light polarization and coherence." *Proc. SPIE vol 8165: Unconventional Imaging, Wavefront Sensing, and Adaptive Coded Aperture Imaging and non-Imaging Sensor Systems*, pp. 816515-816515-12. (2011)
[19] W. Zhang, Y. Cao, X. Zhang *et al.*, “Sky light polarization detection with linear polarizer triplet in light field camera inspired by insect vision,” Applied Optics, 54(30), 8962-8970 (2015).
[20] M. R. Luo, G. Cui, and C. Li, “Uniform colour spaces based on CIECAM02 colour appearance model,” Color Research & Application, 31(4), 320-330 (2006).
[21] N. J. Smith, and S. v. d. Walt, [Viscm: A Colormap Tool], (2015).
[22] N. J. Smith, [Colorspacious: A powerful, accurate, and easy-to-use Python library for doing colorspace conversions], (2016).
[23] M. R. Luo, G. Cui, and B. Rigg, “The development of the CIE 2000 colour-difference formula: CIEDE2000,” Color Research & Application, 26(5), 340-350 (2001).
[24] S. Bezryadin, P. Burov, and I. Tryndin, "Just Noticeable Difference vs Visual Difference - Hypotheses and how to verify their validity." *Proc. SPIE vol 7867*: *Image Quality and System Performance VIII*.pp. 78670Q (2011)
[25] G. Sharma, [Color fundamentals for digital imaging] CRC Press, 1 (2002).
[26] M. Mahy, L. Van Eycken, and A. Oosterlinck, “Evaluation of Uniform Color Spaces Developed after the Adoption of CIELAB and CIELUV,” Color Research & Application, 19(2), 105-121 (1994).
[27] H. Wang, G. Cui, M. R. Luo *et al.*, “Evaluation of colour-difference formulae for different colour-difference magnitudes,” Color Research & Application, 37(5), 316-325 (2012).
[28] I. C. o. Illumination, [CIE S 017/E:2011 ILV: International Lighting Vocabulary], 17-233 (2011).
[29] I. C. o. Illumination, [CIE S 017/E:2011 ILV: International Lighting Vocabulary], 17-1136 (2011).
[30] J. Scott Tyo, B. M. Ratliff, and A. S. Alenin, “Adapting the HSV polarization-color mapping for regions with low irradiance and high polarization,” Optics Letters, 41(20), 4759-4762 (2016).
[31] N. Smith, and S. v. d. Walt, [A Better Default Colormap for Matplotlib] Youtube, (2015).
[32] K. Thyng, [Cmocean: Beautiful colormaps for oceanography], (2015).
[33] K. T. Mullen, W. H. A. Beaudot, and I. V. Ivanov, “Evidence that global processing does not limit thresholds for RF shape discrimination,” Journal of Vision, 11(3), 6-6 (2011).
[34] K. T. Mullen, and W. H. A. Beaudot, “Comparison of color and luminance vision on a global shape discrimination task,” Vision Research, 42(5), 565-575 (2002).
[35] J. Craven-Jones, M. W. Kudenov, M. G. Stapelbroek, and E. L. Dereniak, “Infrared hyperspectral imaging polarimeter using birefringent prisms,” Applied Optics **50**(8) pp. 1170 – 1185 (2011)